Journal of Nuclear Materials 385 (2009) 117–121

Contents lists available at ScienceDirect

Journal of Nuclear Materials

journal homepage: www.elsevier.com/locate/jnucmat

Lattice parameters of (U, Pu, Am, Np)O_{2-x}

Masato Kato [a,*], Kenji Konashi [b]

[a] Fuel Technology R&D Section, Nuclear Fuel Cycle Engineering Laboratories, Japan Atomic Energy Agency, 4-33, Muramatsu, Tokai-mura, Naka-gun, Ibaraki 319-1194, Japan
[b] Tohoku University, 2145-2, Narita, Oarai-machi, Ibaraki 311-1313, Japan

A B S T R A C T

The solid solutions of $(U_{1-z-y'-y''}Pu_zAm_{y'}Np_{y''})O_{2-x}$ (z = 0–1, y' = 0–0.12, y'' = 0–0.07) were investigated by X-ray diffraction measurements, and a database for the lattice parameters was updated. A model to calculate the lattice parameters was derived from the database. The radii of the ions present in the fluorite structure of (U, Pu, Am, Np)O_{2-x} were estimated from the lattice parameters measured in this work. The model represented the experimental data within a standard deviation of σ = ±0.025%.

1. Introduction

Uranium and plutonium mixed oxides (MOX) containing minor actinide elements (MA) have been developed as fuels for advanced fast reactors [1,2]. As a part of the development, previous reports have investigated the effects of MA on physical properties, melting temperatures, thermal conductivities, oxygen potentials, lattice parameters and phase separation [3–10].

Lattice parameters are basic data for expressing material characteristics. In the case of MOX fuels, they have been used to evaluate thermal physical properties such as thermal conductivity and heat capacity. In addition, the theoretical density of MOX has been obtained from lattice parameters and it is used to control the quality of the fuel pellets in the fabrication process. Therefore, lattice parameters are essential data to develop nuclear fuels.

In a previous work [8], the effect of MA content on the lattice parameters of MOX containing about 30%Pu was measured, and the lattice parameter change by Vegard's law was reported. However, data for a broader range of compositions are needed to develop fuels for the advanced fast reactors. In this work, the lattice parameters of (U, Pu, Am, Np)O_{2-x} were investigated, the (U, Pu, Am, Np)O_{2-x} database was updated, and a model to represent the lattice parameters was derived as a function of composition.

2. Experimental procedures

Samples listed in Table 1 were prepared as functions of Pu content, Am content and oxygen-to-metal (O/M) ratio. Raw powders of UO_2, $(U_{0.513}Pu_{0.463}Am_{0.624})O_2$, $(Pu_{0.979}Am_{0.021})O_2$ and $(Pu_{0.926}Am_{0.072})O_2$ were used for preparation of the samples. Americium was yielded by β-decay of ^{241}Pu and accumulated in the powder. The samples were prepared by a mechanical blending method. All samples were confirmed to be homogeneous fcc single phase by X-ray diffraction analyses in the range of 2θ from 10–90° and by electron probe micro analyses, after the samples were adjusted to stoichiometric composition. After that the samples were adjusted to various O/M ratios by annealing in appropriate conditions [9]. Two kinds of samples with O/M ratios of 1.718 and 1.733 of 46% Pu-MOX were prepared by carbothermal reduction. In this reduction, samples were mixed with 2.2–2.6 wt% carbon and heated at 1773 K for 1 h in an atmosphere of 5%H_2/Ar gas mixture.

The X-ray diffraction patterns of samples were measured with an X-ray powder diffractometer (Rigaku RINT-1100 system) within a few days after annealing. For this, each sample was ground in an agate mortar and the powder was put on a glass sample holder. The X-ray diffraction patterns were obtained by Cu Kα radiation through a monochromator. Lattice parameters of a typical fcc structure were obtained by fitting the X-ray diffraction pattern in the range of 2θ from 110–145° by Rietveld analysis [11]. The R_{wp} factor in the analysis was minimized to 8–12%, and the analysis accuracy of the lattice parameter was within ±0.001 Å.

3. Results and discussion

The results of X-ray diffraction measurements are summarized in Table 1. The phase separation [8,12–14] into two fcc phases was observed in some samples with low O/M and Pu content of more than 30%. The effect of the composition change on lattice parameter was evaluated using the data of fcc single phase. Fig. 1(a) and (b) shows X-ray diffraction patterns of 43%Pu-MOX in the range of 2θ = 10–90° and 110–145°. Their patterns were identified as fcc single phase. The lattice parameter was analysed from the pattern shown in Fig. 1(b) and obtained as 5.4358 Å ± 0.0007 Å.

Figs. 2 and 3 show lattice parameters of $(U_{1-z-y}Pu_zAm_y)O_{2.00}$ and $(U_{1-z-2y}Pu_zAm_yNp_y)O_{2.00}$, respectively. The lattice parameters decrease with increasing Am and Np content. The lattice parameter of the fluorite structure is expressed by Eq. (1) from ionic radii,

* Corresponding author. Tel.: +81 29 282 1111; fax: +81 29 282 9473.
E-mail address: kato.masato@jaea.go.jp (M. Kato).

0022-3115/$ - see front matter © 2008 Elsevier B.V. All rights reserved.
doi:10.1016/j.jnucmat.2008.09.037

Table 1
Results of X-ray diffraction measurements.

Sample name	Composition					Results of X-ray diffraction		
	U (%)	Pu (%)	Np (%)	Am (%)	O/M	Lattice parameter (Å)		Phase
MOX-1[8]	70.3	29.0		0.7	2.000	5.4490		fcc
					2.000	5.4482		fcc
					2.000	5.4485		fcc
					2.000	5.4490		fcc
					2.000	5.4479		fcc
					1.997	5.4484		fcc
					1.993	5.4492		fcc
					1.986	5.4496		fcc
					1.980	5.4503		fcc
					1.959	5.4478	5.4569	fcc + fcc
					1.942	5.4507	5.4727	fcc + fcc
					1.932	5.4522	5.4677	fcc + fcc
					1.924	5.4503	5.4718	fcc + fcc
					1.909	5.4495	5.4784	fcc + fcc
MOX-2 [8]	69.5	30.0		0.5	2.000	5.4475		fcc
					1.999	5.4480		fcc
					1.987	5.4514		fcc
					1.981	5.4518		fcc
					1.965	–		fcc + fcc
					1.935	–		fcc + fcc
					1.929	–		fcc + fcc
					1.924	–		fcc + fcc
6%Np–MOX[8,10]	64.3	29.0	6.0	0.7	2.000	5.4463		fcc
					2.000	5.4463		fcc
					2.000	5.4468		fcc
					1.999	5.4465		fcc
					1.998	5.4471		fcc
					1.997	5.4490		fcc
					1.980	5.4500		fcc
					1.957	5.4490	5.4791	fcc + fcc
					1.945	5.4502	5.4864	fcc + fcc
					1.930	5.4504	5.4740	fcc + fcc
					1.927	5.4472	5.4800	fcc + fcc
					1.914	5.4474	5.4849	fcc + fcc
12%Np-MOX[8,10]	58.3	29.0	12.0	0.7	2.000	5.4442		fcc
					2.000	5.4441		fcc
					2.000	5.4440		fcc
					1.998	5.4451		fcc
					1.997	5.4445		fcc
					1.989	5.4464		fcc
					1.987	5.4477		fcc
					1.962	5.4472	5.4776	fcc + fcc
					1.945	5.4473	5.4810	fcc + fcc
					1.931	5.4466	5.4773	fcc + fcc
					1.923	5.4471	5.4703	fcc + fcc
					1.909	5.4470	5.4767	fcc + fcc
2.4%Am-MOX[8]	67.6	30.0	0.0	2.4	2.000	5.4469		fcc
					1.951	5.4480	5.4598	fcc + fcc
2%Np/Am-MOX[8]	66.0	30.0	2.0	2.0	2.000	5.4461		fcc
					2.000	5.4466		fcc
					1.983	5.4470		fcc
					1.976	5.4491		fcc
					1.923	5.4536	–	fcc + fcc
1.8%Np/Am-MOX[8]	66.4	30.0	1.8	1.8	2.004	5.4465		fcc
					2.000	5.4464		fcc
					2.000	5.4466		fcc
					2.000	5.4463		fcc
					1.986	5.4503		fcc
					1.979	5.4515		fcc
					1.964	–	–	fcc + fcc
					1.931	–	–	fcc + fcc
					1.921	–	–	fcc + fcc
					1.919	–	–	fcc + fcc
12%Pu-MOX[9]	87.9	11.8		0.3	2.000	5.4622		fcc
					1.989	5.4632		fcc
					1.983	5.4652		fcc
					1.975	5.4693		fcc
					1.974	5.4699		fcc
					1.971	5.4696		fcc

(*continued on next page*)

Table 1 (*continued*)

Sample name	Composition					Results of X-ray diffraction		
	U (%)	Pu (%)	Np (%)	Am (%)	O/M	Lattice parameter (Å)		Phase
20%Pu-MOX-1[9]	79.7	19.9		0.4	2.000	5.4558		fcc
					1.982	5.4595		fcc
					1.967	5.4626		fcc
					1.950	5.4699		fcc
					1.942	5.4734		fcc
20%Pu-MOX-2*	78.7	19.8		1.5	2.000	5.4538		fcc
					2.000	5.4540		fcc
					1.996	5.4554		fcc
					1.993	5.4559		fcc
					1.988	5.4561		fcc
					1.981	5.4593		fcc
					1.967	5.4637		fcc
					1.961	5.4609		fcc
					1.953	5.4661		fcc
					1.947	5.4707		fcc
MOX-3*	69.6	29.8		0.6	2.000	5.44665		fcc
40%Pu-MOX-1*	59.6	39.7		0.7	2.000	5.4404		fcc
					1.972	5.4449		fcc
					1.959	5.4421	–	fcc + fcc
					1.949	5.4435	–	fcc + fcc
					1.925	5.4458	–	fcc + fcc
					1.916	5.4439	–	fcc + fcc
40%Pu-MOX-2*	58.5	39.6		1.9	2.000	5.4381		fcc
					1.961	5.4473	–	fcc
40%Pu-MOX-3*	58.4	38.3		3.3	2.000	5.4384		fcc
43%Pu-MOX*	53.7	42.8		3.5	2.000	5.4358		fcc
46% Pu-MOX*	51.4	46.3		2.4	2.000	5.4332		fcc
					2.000	5.43391		fcc
					1.976	5.4397		fcc
					1.957	5.4398	–	fcc + fcc
					1.934	5.438	–	fcc + fcc
					1.718	5.5067		fcc
					1.733	5.5032		fcc
60% Pu-MOX*	37.7	60.0		2.3	2.00	5.4247	–	fcc + fcc
2%Am-PuO_2*		97.9		2.1	2.00	5.3960		fcc
6%Am-PuO_2*		93.6		6.4	2.00	5.3944		fcc
7%Am-PuO_2*		94.0		7.2	2.00	5.3975		fcc

* The data were measured in this work.

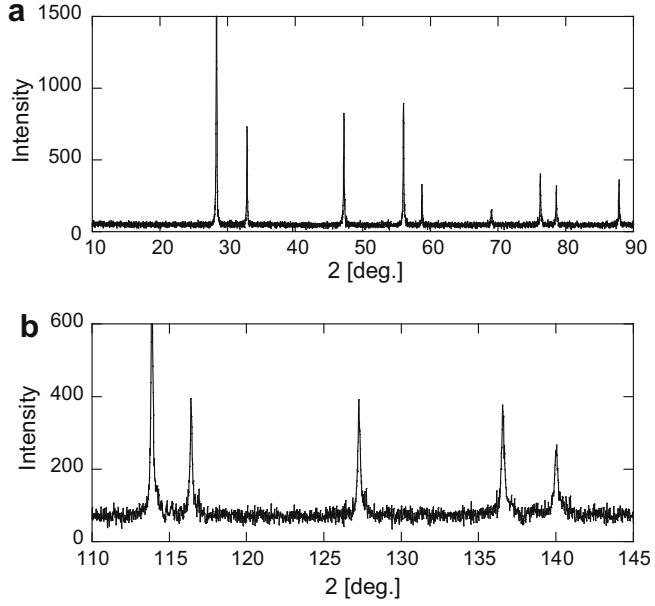

Fig. 1. X-ray diffraction patterns of 43%Pu-MOX in the range of (a) 2θ = 10–90 and (b) 2θ = 110–145.

$$a = 4/\sqrt{3}(r_c + r_e), \quad (1)$$

where a is lattice parameter, r_a is ionic radius of anion and r_c is ionic radius of cation. Ionic radii reported by Shannon [15] are shown in Table 2. It is well-known that ionic radius varies significantly with coordination number (CN) and valence. In the case of the stoichiometric fluorite structure, CNs are 8 for cation and 3 for anion. The lattice parameters of (U, Pu, Am, Np)$O_{2.00}$ shown in Figs. 2 and 3 were fitted by Eq. (1) as a function of the ionic radii. Ionic radius, r_c, was obtained from Eq. (2) in $(U_{1-z-y'-y''}Pu_zAm_{y'}Np_{y''})O_{2.00}$.

$$r_c = r_U(1 - z - y' - y'') + r_{Pu}z + r_{Am}y' + r_{Np}y''. \quad (2)$$

The lines shown in Figs. 2 and 3 were calculated by Eq. (2). The ionic radii obtained from them are given in Table 2. The evaluated ionic radii are in good agreement with those reported by Shannon [15] within ±0.01 Å. The good agreement between the measured and the calculated data suggests that (U, Pu, Am, Np)$O_{2.00}$ is a solid solution.

Fig. 4 shows variation of $r_{(U_{1-z-y}Pu_zAm_y)}/r_{(U_{1-z}Pu_z)}$ with Am content, which was calculated from ionic radius of O^{2-} and the measured lattice parameter using Eq. (1). The lines were calculated for the cases of $(U^{4+}_{0.7-y'}Pu^{4+}_{0.3}Am^{4+}_{y'})O^{2-}_{2.00}$ and $(U^{4+}_{0.7-2y'}U^{5+}_{y'}Pu^{4+}_{0.3}Am^{3+}_{y'})O^{2-}_{2.00}$ [16]. The plotted data lie along the line for $(U^{4+}_{0.7-y'}Pu^{4+}_{0.3}Am^{4+}_{y'})O^{2-}_{2.00}$, and therefore it is considered that the valence of Am is +4 in the stoichiometric oxide. The lattice parameters of (U, Pu, Np)$_{2.00}$ are in good agreement with the values

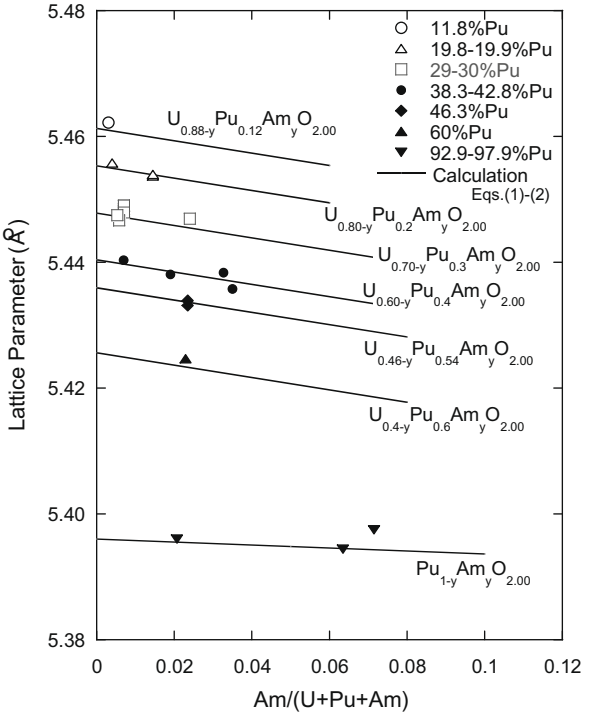

Fig. 2. The effect of Am content on lattice parameters of (U, Pu, Am)$O_{2.00}$.

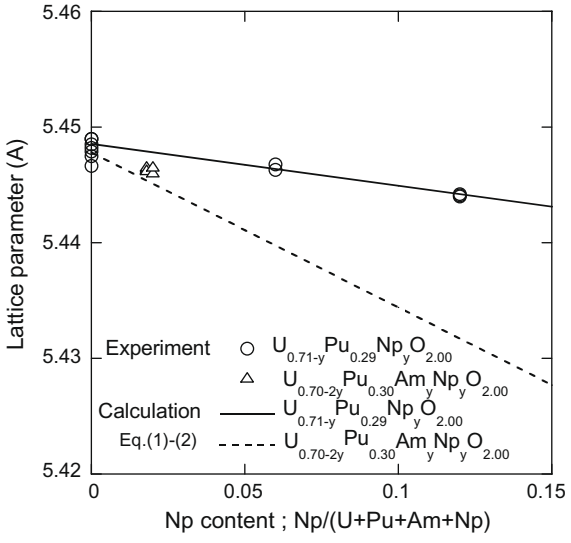

Fig. 3. The lattice parameters of (U, Pu, Am, Np)$O_{2.00}$.

Table 2
Ionic radii.

Ionic species	CN	Ionic radius (Å)	
		Ref. [15]	This work
U^{5+}	8	0.840	–
U^{4+}	8	1.00	0.9972
Pu^{4+}	8	0.96	0.9642
Pu^{3+}	6	1.00	–
Am^{4+}	8	0.95	0.9539
Am^{3+}	8	1.090	–
Am^{3+}	6	0.975	–
Np^{4+}	8	0.98	0.9805
O^{2-}	4	1.38	1.372

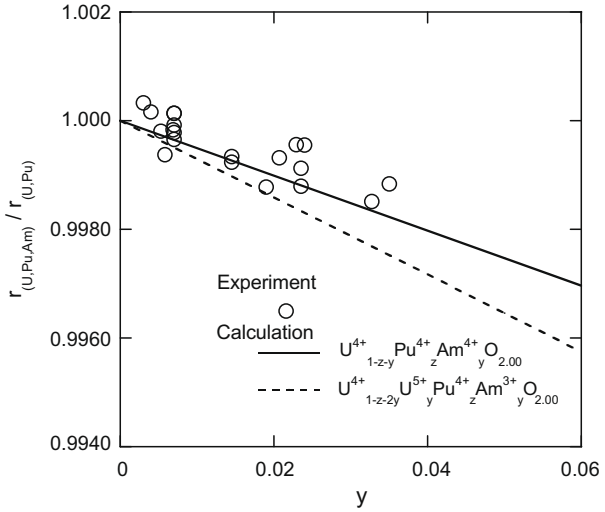

Fig. 4. Variation of ionic radius ratio of cations in (U, Pu, Am)$O_{2.00}$.

obtained from ionic radii of U^{4+}, Pu^{+4} and Np^{4+}, so the valence of Np is +4 in the stoichiometric oxide.

The effect of O/M ratio on the lattice parameters is shown in Fig. 5. In all the samples, the lattice parameters increase with decreasing O/M ratio. Fig. 6 shows the effect of O/M ratio on ionic radius ratio $r_c^{(4-2x)+}/r_c^{4+}$ of cation in (U, Pu, Am, Np)$O_{2.00-x}$. Assuming that the ionic radius $r_c^{(4-2x)+}$ dependence on x is gotten from ionic radii of M^{4+} and M^{3+}, then $r_c^{(4-2x)+}$ was calculated by Eq. (3),

$$r_c^{(4-2x)+} = \left(1 - \frac{x}{1.5}\right) r_{M^{4+}} + \frac{x}{1.5} r_{M^{3+}}, \tag{3}$$

where $r_{M^{4+}}$ and $r_{M^{3+}}$ are ionic radii for CN = 8 and 6, respectively.

The variations of $r_{Am}^{(4-2x)+}/r_{Am}^{4+}$ and $r_{Pu}^{(4-2x)+}/r_{Pu}^{4+}$ are also shown in the figure. The trend seen for the experimental data is comparable with that of $r_{Pu}^{(4-2x)+}/r_{Pu}^{4+}$. The plotted data shown in Fig. 6 were represented by a linear function, and Eq. (4) was obtained. The lattice parameter in $(U_{1-z-y'-y''}Pu_zAm_{y'}Np_{y''})O_{2.00-x}$ could be expressed by Eq. (5)

$$r_c^{(4-2x)+}/r_c^{4+} = 1 + 0.112x, \tag{4}$$

$$a = 4/\sqrt{3}\left[(r_U(1-z-y'-y'') + r_{Pu}z + r_{Am}y' + r_{Np}y'')(1+0.112x) + r_a)\right]. \tag{5}$$

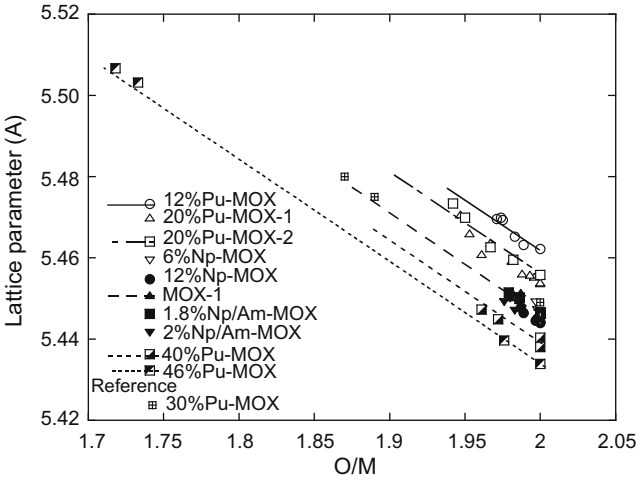

Fig. 5. The effect of O/M ratio on lattice parameters of (U, Pu, Am, Np)$O_{2.00-x}$. The lines were calculated by Eq. (5).

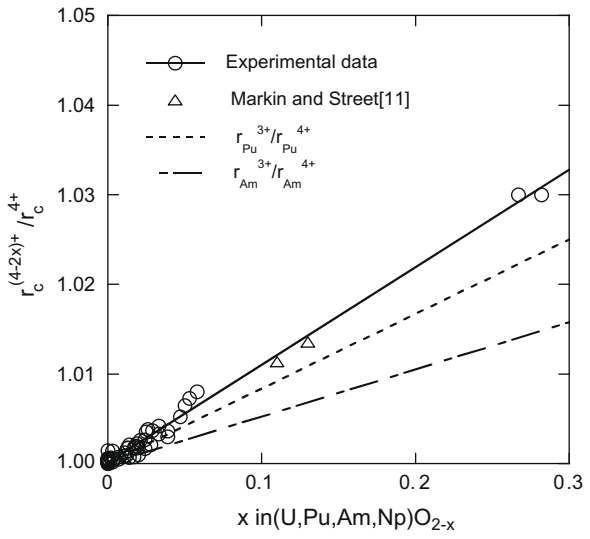

Fig. 6. The effect of O/M ratio on ionic radius ratio of cations in (U, Pu, Am, Np)$O_{2.00-x}$.

The variations calculated by Eq. (5) are shown in Fig. 5, and the derived equation represents the experimental data very well within the standard deviation of $\sigma = 0.025\%$.

Ohmichi et al. [17] derived a model to calculate the lattice parameters of (U, Pu)O_{2-x}, which took into account the size effect of oxygen vacancy. Nakamura et al. [18], however, modeled the lattice parameters of the defect-fluorite oxides by taking into account the ionic radii of CN = 8 and 6. And they reported that the effect of the oxygen vacancy was incorporated in the model. In the present work, the effect of oxygen vacancy was not observed clearly.

4. Conclusion

The solid solutions of $(U_{1-z-y'-y''}Pu_zAm_{y'}Np_{y''})O_{2-x}$ ($z = 0$–1, $y' = 0$–0.12, $y'' = 0$–0.07) were investigated by X-ray diffraction measurements. A database of the lattice parameters of (U, Pu, Np, Am)O_{2-x} was updated over a wide range of compositions. The ionic radii were estimated from lattice parameters, and a model to calculate the lattice parameters was derived as functions of Pu content, MA content and O/M ratio. The derived model represented the experimental data with precision of $\sigma = \pm 0.025\%$. It was considered that Np^{4+} and Am^{+4} were stable in the stoichiometric MOX having a low MA content like the samples evaluated in this work.

Acknowledgements

The authors are pleased to acknowledge Messrs H. Uno, T. Tamura, M. Sugata, T. Sunaoshi and K. Shibata for their collaboration in the sample preparation and analyses.

References

[1] Y. Sagayama, Proc. Global 2007, Boise, Idaho, USA, September 9–13, 2007, p. 251.
[2] H. Funasaka, M. Ito, Proc. Global 2007, Boise, Idaho, USA, September 9–13, 2007, p. 259.
[3] M. Kato et al., J. Nucl. Mater. 373 (2008) 237.
[4] S. Nakamichi et al., Trans. Am. Nucl. Soc. 96 (2007) 191.
[5] K. Morimoto et al., J. Nucl. Mater. 374 (2007) 378.
[6] M. Kato et al., Trans. Am. Nucl. Soc. 91 (2004) 463.
[7] K. Morimoto et al.T. Abe, J. Alloys Comp. 444–445 (2007) 590.
[8] M. Kato et al., Recent Adv. Actinide Sci. (2006) 367.
[9] M. Kato et al., J. Alloys Comp. 452 (2008) 48–53.
[10] K. Morimoto et al., Global 2001, Paris, September 9–13, 2001, p. 38.
[11] F. Izumi et al., Physica C 335 (2000) 239.
[12] T.L. Markin, R.S. Street, J. Inorg. Nucl. Chem. 29 (1967) 2265.
[13] T.L. Markin, E.J. McIver, Plutonium 1965, Chapman and Hall, London, 1967. p. 845.
[14] C. Sari et al., J. Nucl. Mater. 35 (1970) 267.
[15] R.D. Shannon, Acta Cryst. A32 (1976) 751.
[16] K. Mayer, B. Kanellakopoulos, J. Naegele, L. Koch, J. Alloys Comp. 213/214 (1994) 456.
[17] T. Ohmichi et al., J. Nucl. Mater. 10 (1981) 40.
[18] A. Nakamura et al., Pure Appl. Chem. 79 (10) (2007) 1691.